Journal of Mineralogical and Petrological Sciences, Volume 98, page 118-129, 2003

Niigataite, $CaSrAl_3(Si_2O_7)(SiO_4)O(OH)$: Sr-analogue of clinozoisite, a new member of the epidote group from the Itoigawa-Ohmi district, Niigata Prefecture, central Japan

Hiroshi MIYAJIMA*, Satoshi MATSUBARA**, Ritsuro MIYAWAKI** and Kazuo HIROKAWA***

**Fossa Magna Museum, Miyama Park, Itoigawa, Niigata 941-0056, Japan*
***Department of Geology, National Science Museum, Hyakunincho, Shinjuku, Tokyo 169-0073, Japan*
****Suihodo Co. Ltd., Suzawa, Ohmi, Niigata 949-0301, Japan*

Niigataite, $CaSrAl_3(Si_2O_7)(SiO_4)O(OH)$, is a new member of the epidote group. It is monoclinic, $P2_1/m$, $a = 8.890(4)$, $b = 5.5878(18)$, $c = 10.211(4)$ Å, $b = 115.12(3)°$, $V = 459.3(3)$ Å^3 and $Z = 2$. The 8 strongest X-ray powder diffractions are d_{obs}(Å)(I/I_0)(hkl): 2.90(100)(11$\bar{3}$), 2.79(48)(020), 2.70(26)(013), 3.22(25)(201), 2.11(24)(221), 2.60(24)(31$\bar{1}$), 5.05(23)(10$\bar{2}$) and 1.397(22)(040). Electron microprobe analysis gave the composition SiO_2 35.49, TiO_2 0.75, Al_2O_3 24.86, Fe_2O_3 7.08, MnO 0.22, MgO 0.07, CaO 14.09, SrO 14.75, H_2O(calc.) 1.77 total 99.08 wt%, corresponding to a formula $Ca_{1.00}(Sr_{0.72}Ca_{0.28})_{\Sigma 1.00}(Al_{2.48}Fe_{0.45}Ti_{0.05}Mn_{0.02}Mg_{0.01})_{\Sigma 3.01}Si_{3.00}O_{13}$. H calculated on the basis of H = 1 and O = 13 per unit formula. It is transparent, pale gray with a yellowish green tint. Cleavage is perfect on one direction. Streak is white. The Vickers microhardness is 642-907 kg/mm^2 (100g load) corresponding to Mohs' 5-5.5. The calculated density is 3.63 g/cm^3. It occurs as anhedral grains in close association with chlorite and diaspore in druse of prehnite rock in the seashore of Miyabana, Ohmi Town, Niigata Prefecture, central Japan. Niigataite is considered to be crystallized under the presence of Sr-rich metamorphic solution in the late stage of the formation of prehnite rock. Sr enrichment is caused by crystallization of prehnite, which is the most abundant phase having no acceptability of Sr.

Introduction

The epidote group minerals occur in a wide variety of parageneses. Based on crystal symmetry, the epidote-group minerals are divided into monoclinic and orthorhombic groups. Common members of the monoclinic one are clinozoisite, epidote, piemontite and allanite-(Ce). Zoisite is the only orthorhombic species in the group. Calcium atoms occupy two different sites in the monoclinic structure: ninefold-coordinated $A(1)$ and tenfold-coordinated $A(2)$ sites. The $A(1)$ site is slightly smaller than the $A(2)$ site. The size of $A(2)$ site is suitable for Sr (1.32 Å) rather than of Ca (1.28 Å) (Dollase, 1971). Because of this crystallochemical feature, Sr is not a rare component in the group; however, Sr content is less than that of Ca in $A(2)$ site except for strontiopiemontite from Val Graveglia, Italy (Bonazzi et al., 1990).

The Itoigawa-Ohmi district (Fig. 1a) is known for the first locality jade found in Japan (Kawano, 1939). The district is located in the easternmost part of the Renge belt (Nishimura, 1998) that is the oldest of the high-P/T metamorphic belts in Japanese Islands (Fig. 1b). During mineralogical studies on jade in the Itoigawa-Ohmi district, we noticed a peculiar coarse-grained purplish rock (Fig. 2a). The rock is essentially composed of prehnite with minor diaspore, chlorite and niigataite. The mineral and its name have been approved by the IMA Commission on New Mineral and Mineral Names (#2001-055). The mineral is named for the locality, Niigata Prefecture. The type specimens of niigataite have been deposited in the National Science Museum, Tokyo (NSM M-28297) and at Fossa Magna Museum, Itoigawa, Niigata (FMM01336).

Occurrence

Niigataite was found in a boulder of the prehnite rock with purple to beige in color from the Miyabana shore, Ohmi Town, Niigata Prefecture (Fig. 1a). The similar rock was also found from the bed of the Ohmi-gawa river, Ohmi Town. The Itoigawa-Ohmi district of the Renge belt is characterized by a serpentinite melange with such high-P/T metamorphic rocks as schists, jadeitite, albitite, rodingite and metagabbro, with

H. Miyajima, m@e-hisui.com Corresponding author
S. Matsubara, matubara@kahaku.go.jp
R. Miyawaki, miyawaki@kahaku.go.jp

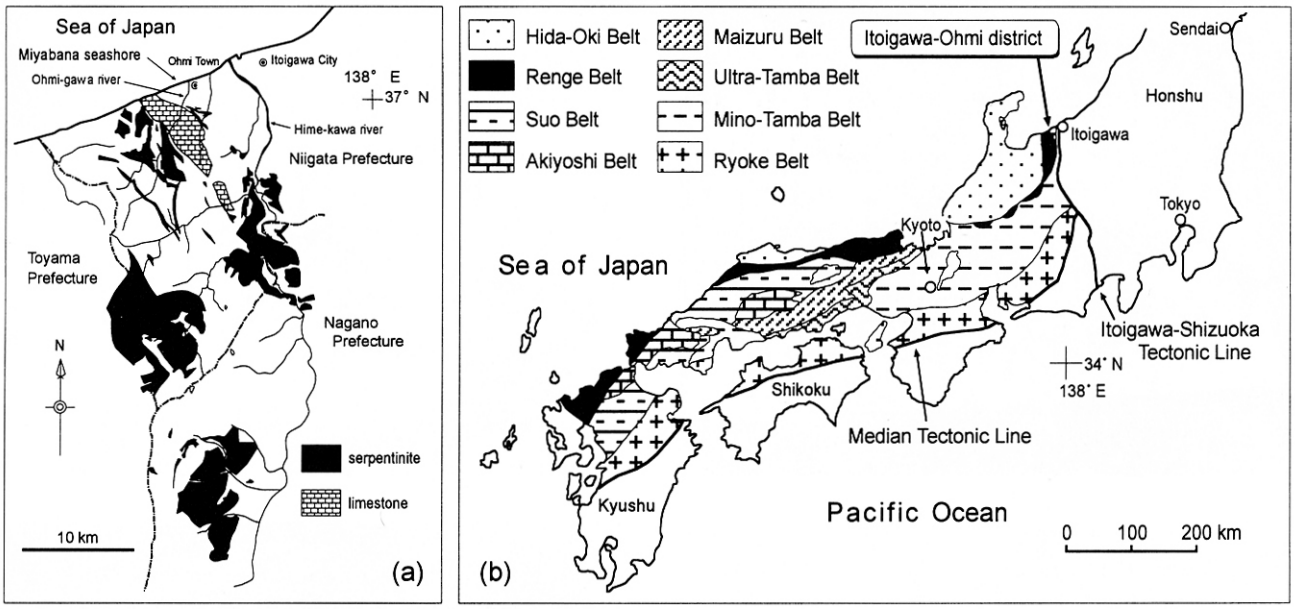

Figure 1. (a) Index map of the Itoigawa-Ohmi district (modified from Komatsu, 1990). (b) Geotectonic subdivision of Southwest Japan (modified from Nishimiura, 1998). The Renge Belt is typically associated with meta-ophiolite sequences (470-340 Ma) including serpentinite. It is also characterized by association of glaucophane-schist.

various fragments of Paleozoic accretionary complexes composed of greenstone, limestone, chert and mudstone (Nakajima et al., 1992). Niigataite-bearing prehnite rock might be included in the serpentinite melange as tectonic blocks.

The niigataite-bearing prehnite rock is composed of fan shaped aggregates of platy prehnite crystals up to 3 cm long (Fig. 2b). Long prismatic to acicular euhedral diaspore crystals up to 1 mm long are found in druse between prehnite crystals. Other minor constituents are chlorite, zircon, galena, cinnabar, niigataite-clinozoisite series minerals. Niigataite is found as subhedral grains approximately 0.5 mm across, and occurs interstitially within chlorite (Fig. 2, c and d). In the other case, niigataite closely associates with Sr-bearing clinozoisite (Fig. 2e). Both of them are indistinguishable under the polarization-microscope.

Physical and optical properties

Niigataite is transparent pale gray with yellowish green tint vitreous luster. It shows violet anomalous

Table 1. The comparison of physical and optical data for the niigataite, strontiopiemontite and clinozoisisite

	Niigataite	Strontiopiemontite	Clinozoisite
Color	pale gray with yellowish green tint	deep red	colorless, pale yellow gray green
Hardness (Mohs)	5.5-6	6	6.5
Density (g/cm^3)	3.63	3.73	3.36
Cleavage	perfect on one direction	perfect on (001)	perfect on (001)
Tenacity	brittle	no data	brittle
Color in thin section	colorless	yellow - reddish violet	colorless
Anomalous interference color	violet	no data	violet
Luster	vitreous	vitreous	vitreous
Streak	white	purple - brown	white
Fluorescence	non observed	non observed	non observed
Refractive indices			
α	not determined	not determined	1.670-1.718
β	not determined	not determined	1.670-1.725
γ	not determined	not determined	1.690-1.734
	$1.67 < n < 1.725$	$n = 1.763$	
2V (°)	not determined	not determined	14 - 90
Reference	this study	Bonazzi et al. (1990)	Deer et al. (1997)

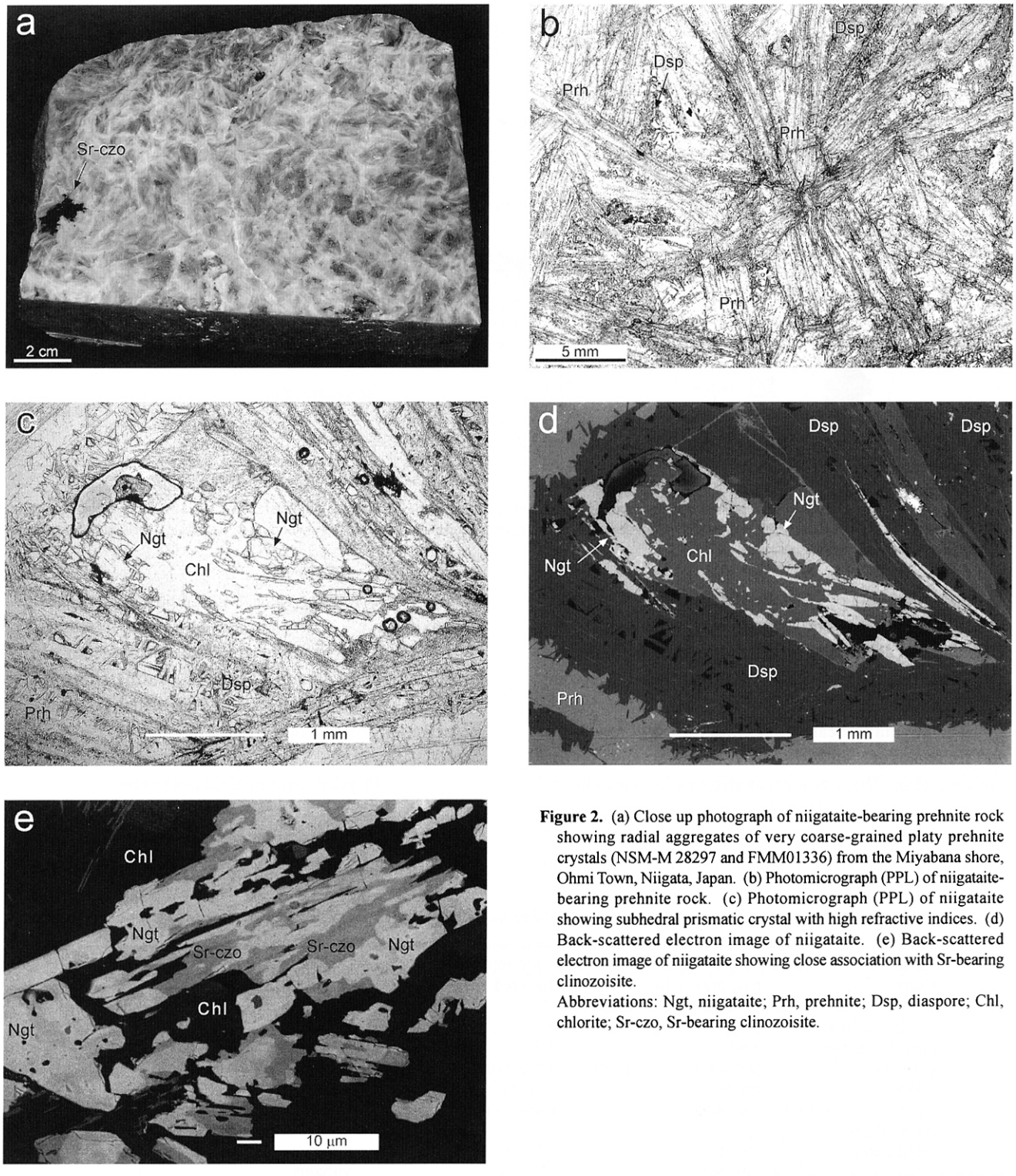

Figure 2. (a) Close up photograph of niigataite-bearing prehnite rock showing radial aggregates of very coarse-grained platy prehnite crystals (NSM-M 28297 and FMM01336) from the Miyabana shore, Ohmi Town, Niigata, Japan. (b) Photomicrograph (PPL) of niigataite-bearing prehnite rock. (c) Photomicrograph (PPL) of niigataite showing subhedral prismatic crystal with high refractive indices. (d) Back-scattered electron image of niigataite. (e) Back-scattered electron image of niigataite showing close association with Sr-bearing clinozoisite.
Abbreviations: Ngt, niigataite; Prh, prehnite; Dsp, diaspore; Chl, chlorite; Sr-czo, Sr-bearing clinozoisite.

interference color. Perfect cleavage was observed on one direction. The Vickers microhardness is 642-907 kg/mm^2 (100g load), corresponding to 5-5.5 on the Mohs' scale. The density could not be measured due to insufficient amount of material. The calculated density is 3.63 g/cm^3. No fluorescence was observed under long or short wave ultraviolet radiation. The refractive indices are between 1.67 (γ of prehnite) and 1.725 (immersion liquid), however, the precise measurement could not be carried out due to small amount of material. The physical and optical data for niigataite, strontiopiemontite and clinozoisite are compared in Table 1.

Chemical composition

Chemical composition of minerals

Chemical analyses of minerals were using a SEM (JEOL JSM-5400) with Link QX 2000 energy dispersive X-ray spectrometer (EDS). Operating conditions are 2-3 μm beam diameter, 15 kV, 10 nA probe current, and standard ZAF correction. Standard materials are Mg_2SiO_4 (for Mg), sillimanite (for Al), wollastonite (for Si and Ca), TiO_2 (for Ti), tephroite (for Mn), Fe_2SiO_4 (for Fe) and SrF_2 (for Sr). The results of the analyses are given in Table 2. Since the water content of niigataite could not be measured due to insufficient quantity of mineral, it was estimated by calculation on the basis of H = 1 and O = 13 in one formula unit. The average of 9 analyses (Table 2) leads to the empirical formula $Ca_{1.00}(Sr_{0.72}\ Ca_{0.28})_{\Sigma 1.00}(Al_{2.48}\ Fe_{0.45}\ Ti_{0.05}\ Mn_{0.02}\ Mg_{0.01})_{\Sigma 3.01}\ Si_{3.00}\ O_{13}\ H$. The ideal formula is $CaSrAl_3(Si_2O_7)(SiO_4)O(OH)$. The back-scattered electron image (Fig. 2e) indicates that chemical variation between niigataite and associated Sr-clinozoisite is not continuous. The SrO range of associated Sr-bearing clinozoisite is from 2.2 to 6.5 wt%, but those of niigataite ranges from 13.9 to 16.8 wt%.

Chemical compostion of rocks

The powdered sample of niigataite-bearing prehnite rock was analyzed for 20 elements, using a wave-length dispersive X-ray fluorescence spectrometer (Rigaku RIX 2000) at Fossa Magna Museum. Operating conditions are 50kV and 50mA. Glass bead made from finely ground sample, was prepared with sample to lithium metaborate flux ratio of 1:10 and analyzed for major elements (Si, Ti, Al, Fe, Mn, Mg, Ca, Na, K and P) using fundamental parameter methods, whereas trace elements (Ce, Cr, Nb, Ni, Pb, Rb, Sr, Th, Y and Zr) were determined using pure press pellets and the empirical calibration curve method (Murata, 1993). The data of first 10 elements were recalculated for total = 100 percent. The results of bulk chemical composition are given in Table 3. The host rock of niigataite mainly consists of prehnite. The chemical composition of prehnite $Ca_2Al_2Si_3O_{10}(OH)_2$ gives SiO_2 43.71, Al_2O_3 24.72, CaO 27.20 and H_2O+ 4.37 (wt%), corresponding to SiO_2 45.71, Al_2O_3 25.84 and CaO 28.44 (wt%) after recalculation to water free composition. Each value except Al_2O_3 is higher than that of niigataite-bearing prehnite rock, because it contains some accessory minerals such as diaspore. The bulk chemical composition of niigataite-bearing prehnite rock is characterized by high concentration of Al_2O_3 and CaO, low SiO_2, and absence of MnO, Na_2O, K_2O and P_2O_5. It is worth noting that the rock is very rich in Sr (1600 ppm).

Crystallography

A single crystal of niigataite was picked up from the thin section, used for chemical analysis, under a binocular microscope. The powder X-ray diffraction pattern for niigataite was obtained using a Gandolfi camera of 114.6 mm diameter employing Ni-filtered Cu$K\alpha$ radiation. The data were recorded on an Imaging Plate, and processed with a Fuji BAS-2500 bio-imaging analyzer using a computer program by Nakamuta (1999) (Table 4). The unit cell parameters refined from the data with Si internal standard (NBS, #640b) were obtained using a computer program by Toraya (1993) are; a = 8.890(4), b = 5.5878(18), c = 10.211(4) Å, β = 115.12(3)° and V = 459.3(3) Å^3. It is monoclinic, space group $P2_1/m$ and Z = 2.

Table 2. Chemical composition of niigataite and Sr-bearing clinozoisite from Itoigawa-Ohmi district, Japan

	Niigataite			Sr-bearing clinozoisite		
	average[1]	max[2]	min[3]	average[4]	max[5]	min[6]
SiO_2	35.49	35.49	35.96	38.73	38.41	39.42
TiO_2	0.75	0.72	0.33	0.00	0.00	0.00
Al_2O_3	24.86	23.36	26.30	31.34	31.36	31.73
Fe_2O_3	7.08	9.49	5.50	1.20	0.42	1.19
MnO	0.22	0.00	0.50	0.00	0.00	0.00
MgO	0.07	0.00	0.00	0.00	0.00	0.00
CaO	14.09	13.39	14.83	22.09	21.11	24.20
SrO	14.75	16.33	13.86	4.34	6.54	2.16
H_2O calc.	1.77	1.77	1.79	1.92	1.91	1.96
Total	99.08	100.55	99.07	99.63	99.74	100.65
formula on the basis of O = 12.5 and H = 1						
Si	2.998	3.000	3.007	3.018	3.017	3.015
Ti	0.048	0.046	0.021	0.000	0.000	0.000
Al	2.475	2.327	2.592	2.879	2.903	2.860
Fe	0.450	0.603	0.346	0.071	0.025	0.068
Mn	0.016	0.000	0.035	0.000	0.000	0.000
Mg	0.008	0.000	0.000	0.000	0.000	0.000
Ca	1.275	1.213	1.329	1.844	1.777	1.983
Sr	0.722	0.800	0.672	0.196	0.298	0.096
H	1.000	1.000	1.000	1.000	1.000	1.000
Total cation	8.992	8.989	9.003	9.007	9.019	9.021
$A(1)$ = Ca	1.000	1.000	1.000	1.000	1.000	1.000
$A(2)$ = Ca	0.275	0.213	0.329	0.844	0.777	0.983
$A(2)$ = Sr	0.722	0.800	0.672	0.196	0.298	0.096
Total $A(2)$	0.998	1.013	1.036	1.040	1.075	1.079
XSr	0.724	0.790	0.671	0.188	0.277	0.089
$A(1) + A(2)$	1.998	2.013	2.036	2.040	2.075	2.079
Total M	2.997	2.976	2.959	2.949	2.928	2.928
XFe	0.150	0.203	0.117	0.023	0.008	0.024

XSr = Sr/(Sr + Ca($A(2)$)), Total M = Al+Fe+Ti+Mn+Mg, XFe = Fe/(Al+Fe+Ti+Mn+Mg). [1]average of 9 analyses, [2]most Sr-rich niigataite, [3]most Sr-poor niigataite, [4]average of 13 analyses, [5]most Sr-rich clinozoisite, [6]most Sr-poor clinozoisite.

Table 3. Bulk chemical composition of leucoclatic rocks as tectonic block within serpentinite melange from the Itoigawa-Ohmi district

Major elements (wt.%)		SiO_2	TiO_2	Al_2O_3	Fe_2O_3	MnO	MgO	CaO	Na_2O	K_2O	P_2O_5
Prehnite rock		38.84	0.43	35.39	0.58	0.00	0.69	24.07	0.00	0.00	0.00
Rodingite		43.17	0.12	24.79	1.45	0.03	1.71	27.93	0.00	0.77	0.03
Green jadeitite	average	59.14	0.03	21.71	0.98	0.01	1.50	3.21	13.22	0.19	0.01
	max	66.52	0.09	24.26	3.59	0.02	3.30	7.98	15.61	0.79	0.02
	min	56.00	0.01	18.02	0.13	0.00	0.27	0.81	10.07	0.00	0.00
Lavender jadeitite	average	57.54	0.41	21.84	0.55	0.00	0.77	4.54	14.16	0.11	0.06
	max	59.29	1.55	22.85	1.21	0.01	2.36	5.51	14.98	0.42	0.46
	min	55.49	0.04	21.10	0.27	0.00	0.26	3.76	12.24	0.00	0.00
Blue jadeitite	average	57.44	0.20	21.77	1.81	0.01	1.75	3.77	13.09	0.12	0.02
	max	61.11	0.45	23.71	4.16	0.03	5.78	11.29	15.05	0.38	0.05
	min	53.09	0.07	16.16	0.25	0.00	0.73	0.99	9.27	0.01	0.00
Albitite	average	74.54	0.05	14.52	0.95	0.02	0.50	0.69	8.32	0.39	0.01
	max	74.74	0.09	15.46	1.18	0.07	0.70	1.04	9.02	1.02	0.02
	min	74.35	0.03	13.99	0.69	0.00	0.16	0.41	7.15	0.08	0.01

Trace elements (ppm)		Ce	Cr	Nb	Ni	Pb	Rb	Sr	Th	Y	Zr
Prehnite rock		20.8	2.0	2.0	8.3	25.2	2.4	1606	2.9	9.0	168.0
Rodingite		32.3	18.5	2.6	36.0	1.1	17.3	276	3.2	10.4	116.3
Green jadeitite	average	4.1	38.6	0.5	41.2	0.9	5.4	499	2.6	9.3	42.2
	max	13.5	116.9	4.1	134.9	6.1	13.5	1275	2.9	9.6	221.5
	min	0.0	6.3	0.0	8.7	0.0	2.6	16	2.2	9.0	4.5
Lavender jadeitite	average	28.4	7.0	22.0	11.0	2.4	4.9	973	2.4	9.3	336.6
	max	73.3	31.3	141.6	61.7	5.8	10.5	3663	2.7	10.2	751.3
	min	3.1	0.2	0.6	0.6	0.5	3.1	284	2.1	8.6	53.3
Blue jadeitite	average	31.3	12.5	4.2	43.4	0.6	4.8	932	3.9	9.4	126.4
	max	88.4	40.0	13.8	259.0	3.1	9.4	4155	6.4	9.8	347 3
	min	4.7	0.0	0.8	9.5	0.0	2.8	103	2.4	8.3	19.5
Albitite	average	7.6	8.7	1.2	9.4	13.4	8.1	383	2.9	12.3	18.4
	max	13.0	16.6	2.1	12.7	36.2	18.6	430	3.6	18.6	33.0
	min	4.2	0.3	0.4	2.7	2.0	2.8	302	2.5	9.1	10.2

The X-ray intensity data were collected with a Rigaku RASA-7R 4-circle diffractometer using graphite monochromatized Mo$K\alpha$ radiation (56 kV, 270 mA). Experimental details pertaining to collection of single-crystal X-ray diffraction data are given in Table 5. The data reductions to F_o^2 with corrections for Lorentz, polarization and absorption (ψ-scan procedure) were made with a computer program by Dr. Kazumasa Sugiyama of the University of Tokyo (personal communication). The atomic positional parameters of clinozoisite (Dollase, 1968) were used as the initial parameters. The computer program, SHELXL-97 (Sheldrick, 1997), was employed for the refinement of crystal structure. Scattering factors for neutral atoms and anomalous dispersion factors were taken from the International Tables for Crystallography, Volume C (1992). Full-matrix least-squares refinement was performed by adjusting positional parameters, scale factor, and displacement parameters.

The occupancy for $A(1)$ site was fixed to be 1.0 Ca. The scattering curves for Sr and Ca were introduced to the $A(2)$ site. The ratio of Sr and Ca in the $A(2)$ site was fixed according to the result of chemical analysis. The occupancy parameters for $M(1)$, $M(2)$ and $M(3)$ sites were refined with constraint of Al + Fe = 1. In further refinements, the positional and isotropic displacement parameters of H atom, which was observed as a differential Fourier peak near the O(10) site, were refined with positional and anisotropic displacement parameters of the other sites. The final atomic coordinates with displacement parameters and interatomic distances are given in Tables 6 and 7, respectively. The final anisotropic displacement parameters and the Fo-Fc table can be obtained from the third author (R. M.).

Discussion

Relationship to other epidote group minerals

The general formula of epidote group minerals is written as $A(1)A(2)M(1)M(2)M(3)(Si_2O_7)(SiO_4)O(OH)$, where $A(1)$ = Ca; $A(2)$ = Ca, Sr, REE, Pb; $M(1)$ = Al, Fe, Mn,

Table 4. Powder X-ray diffraction data for niigataite and clinozoisite

			Niigataite Niigata, Japan (Presentstudy)			Clinozoisite Rila Mountain, Bulgaria (Macicek et al., 1991)					Niigataite Niigata, Japan (Presentstudy)		Clinozoisite Rila Mountain, Bulgaria (Macicek et al., 1991)		
h	*k*	*l*	I/I_0	$d_{obs.}$	$d_{calc.}$	I/I_0	$d_{obs.}$	*h*	*k*	*l*	I/I_0	$d_{obs.}$	$d_{calc.}$	I/I_0	$d_{obs.}$
0	0	1	3	9.29	9.25	1	9.16	4	2	-3			1.706	1	1.708
1	0	0	3	8.05	8.05	4	8.03	2	0	-6			1.700	2	1.689
1	0	-2	23	5.05	5.04	9	5.02	3	0	-6	3	1.679	1.679	2	1.671
0	1	1	9	4.78	4.78	1	4.78	1	0	-6	7	1.648	1.648	12	1.636
1	1	0	3	4.59	4.59	1	4.59	2	1	4			1.639	2	1.627
1	1	-1			4.58	1	4.59	5	1	-1			1.638	12	1.636
2	0	0	9	4.02	4.02	3	4.01	1	3	-3	18*	1.632	1.634		
2	0	-2			3.99	2	3.99	4	2	0			1.633		
1	1	1	6	3.76	3.76	7	3.75	1	2	4			1.630	12	1.623
0	1	2	2	3.56	3.56			5	1	-4			1.629	2	1.627
2	1	-1	18	3.48	3.48	11	3.48	2	1	-6			1.626	6	1.617
1	0	2	5	3.43	3.43	11	3.40	1	2	-5			1.624	6	1.617
2	0	1	25	3.22	3.22	7	3.20	4	2	-4			1.623	12	1.623
0	0	3	4	3.09	3.08	11	3.05	3	2	2	8	1.618	1.617		
3	0	-1	1	2.99	2.93			5	0	-5			1.595	1	1.594
3	0	-2			2.92	10	2.92	0	3	3			1.594	1	1.594
1	1	-3	100	2.90	2.90	100	2.89	4	0	-6	16	1.592	1.592	2	1.587
0	2	0	48	2.79	2.79	47	2.80	1	1	5			1.587	8	1.575
2	1	1			2.79	10	2.78	3	3	-1	3	1.572	1.572	8	1.575
0	1	3	26	2.70	2.70	24	2.68	4	1	2	9	1.548	1.549	5	1.540
3	0	0			2.68	20	2.67	5	1	0			1.547	2	1.543
0	2	1			2.67	24	2.68	0	0	6			1.541	2	1.528
1	2	0	18	2.64	2.64	6	2.65	3	3	-3			1.525	2	1.528
3	1	-1	24	2.60	2.60	6	2.60	2	2	4			1.461		
2	0	2	15	2.55	2.55	18	2.53	5	2	-1			1.461	5	1.459
1	0	-4	9	2.52	2.52	24	2.51	6	0	-4	3	1.462	1.460	5	1.459
2	0	-4			2.52	24	2.51	5	2	-4	10	1.453	1.454	1	1.454
1	2	-2	11	2.44	2.44	2	2.45	2	2	-6			1.452		
3	1	-3	21	2.40	2.40	12	2.40	3	3	-4			1.447	1	1.448
0	2	2			2.39	34	2.39	3	2	-6	5	1.439	1.439	1	1.448
2	2	-1	2	2.37	2.37	2	2.37	4	0	3	3	1.429	1.430		
0	0	4			2.31			2	1	5	3	1.414	1.414		
1	1	-4			2.30			3	1	-7			1.408	7	1.401
3	0	-4			2.30	8	2.29	1	0	-7			1.402	6	1.391
2	2	-2	7	2.29	2.29	8	2.29	0	4	0	22	1.397	1.397	7	1.401
4	0	-1	5	2.16	2.17	26	2.16	4	2	2			1.396	6	1.391
1	2	2			2.17	26	2.16	4	2	-6	1	1.383	1.384		
4	0	-3			2.15			1	3	4	3	1.365	1.365	1	1.350
0	1	4	3	2.14	2.14	3	2.12	1	1	-7			1.360	1	1.350
2	2	1	24	2.11	2.11	6	2.11	5	0	2			1.352	1	1.345
2	2	-3			2.10	17	2.10	0	2	6	4	1.349	1.349	1	1.341
0	2	3	11	2.07	2.07	6	2.06	6	2	-3	2	1.309	1.309		
4	1	-2			2.06	6	2.06	6	2	-2	4	1.294	1.298		
2	0	3			2.06	13	2.04	6	2	-4			1.294	1	1.295
2	0	-5	2	2.04	2.04			1	4	2			1.294	1	1.295
3	2	-1			2.02	1	2.02	6	1	-6			1.293	1	1.292
3	2	-2			2.02			4	3	-5			1.292	1	1.292
4	0	0	8	2.01	2.01	3	2.01	3	0	5			1.288	1	1.275
4	1	-3			2.01	4	2.01	0	1	7			1.285		
1	0	4			2.01	4	1.989	5	3	-2	3	1.283	1.284		
3	0	-5	5	1.959	1.960	2	1.952	3	0	-8			1.276		
1	1	4			1.889	7	1.876	4	0	4			1.273	3	1.264
2	2	2	16	1.883	1.882	9	1.878	4	2	3	8	1.273	1.273	1	1.267
1	1	-5			1.880	8	1.868	7	0	-3			1.268	1	1.267
4	1	-4			1.878	7	1.876	2	0	-8	6	1.262	1.262	1	1.253
1	2	-4			1.873	8	1.868	5	3	-1			1.261		
2	2	-4	21	1.872	1.871			3	4	-1			1.261	3	1.264
3	1	2			1.869	2	1.860	3	4	-2			1.260		
1	3	0	1	1.814	1.815			6	2	-5	6	1.257	1.256		
0	2	4	2	1.781	1.781			2	3	-6			1.256	1	1.253
5	0	-2			1.772	1	1.771	3	4	0	3	1.238	1.239		
0	1	5	1	1.754	1.756	3	1.743	2	1	6			1.239	1	1.228
2	3	-1	4	1.717	1.718	2	1.722	1	3	5			1.237		
2	0	4			1.715	2	1.700	2	4	2	4	1.225	1.225		
4	1	-5	8	1.706	1.707	2	1.704	6	1	-7	2	1.211	1.211		

*Estimated from data with the external Si-standard, beacause of overlap by the diffraction of Si-standard.

Table 5. Crystallographic data for niigataite derived from the single-crystal X-ray diffraction analysis and experimental details

a (Å)	8.882(3)	2θ range	5.0 - 75.0
b (Å)	5.5906(16)	Reflection range	$6 \leq h \leq 15, -9 \leq k \leq 4, -17 \leq l \leq 15$
c (Å)	10.210(2)	No. of measured reflections	3073
β (°)	115.118(18)	No. unique reflections	2598
V (Å^3)	459.1(2)	No. of observed reflections	
		$[F_o^2 > 2\sigma(F_o^2)]$	1744
Space group	$P2_1/m$	R_{int}	0.0415
Z	2	Variable parameters	124
Formula	$(Sr,Ca)Ca(Al,Fe)_3(Si_2O_7)(SiO_4)O(OH)$	$R1$ $[F_o^2 > 2\sigma(F_o^2)]$	0.0453
$D_{calc.}$ (g/cm^3)	3.643	$R1$(all reflections)	0.0900
μ (cm^{-1})	6.488	$wR2$ (all reflections)	0.1746
Crystal dimension (mm)	0.03 x 0.03 x 0.01	Weighting parameters, a, b	0.1, 0
Diffractometer	Rigaku AFC-7R	Goodness of fit	1.143
Radiation	Mo$K\alpha$ (graphite)	Final $\Delta\rho_{min}$ (e/Å^3)	-2.371
Scan mode, rate (°/min in ω)	2θ-ω, 4	Final $\Delta\rho_{max}$ (e/Å^3)	1.28

$R1 = \Sigma \mid |F_o| - |F_c| \mid / \Sigma |F_o|$
$wR2 = \Sigma [w(F_o^2 - F_c^2)^2] / \Sigma [w(F_o^2)^2]^{0.5}$
$w = 1 / [\sigma^2(F_o^2) + (aP)^2 + bP]$
$P = [2F_c^2 + F_o^2] / 3$

Table 6. Final atomic coordinates, equivalent isotropic displacement parameters, and occupancy parameters

	x	y	z	U_{eq}	Occ.
A(1)	0.76449(13)	0.75	0.15723(10)	0.00851(18)	1Ca
A(2)	0.59833(8)	0.75	0.42171(7)	0.01384(16)	0.72Sr + 0.28Ca
M(1)	0	0	0	0.0061(4)	0.042(9)Fe + 0.958Al
M(2)	0	0	0.5	0.0059(4)	0.025(8)Fe + 0.975Al
M(3)	0.28705(16)	0.25	0.22059(14)	0.0072(3)	0.193(8)Fe + 0.807Al
Si(1)	0.33742(17)	0.75	0.04542(14)	0.0042(2)	1Si
Si(2)	0.68025(17)	0.25	0.27702(14)	0.0048(2)	1Si
Si(3)	0.17874(17)	0.75	0.31274(14)	0.0045(2)	1Si
O(1)	0.2346(3)	0.9966(4)	0.0462(3)	0.0066(4)	1O
O(2)	0.2966(3)	0.9858(4)	0.3465(3)	0.0070(4)	1O
O(3)	0.7879(3)	0.0124(4)	0.3483(3)	0.0082(4)	1O
O(4)	0.0535(4)	0.25	0.1301(4)	0.0052(5)	1O
O(5)	0.0369(4)	0.75	0.1426(4)	0.0055(5)	1O
O(6)	0.0594(4)	0.75	0.3997(4)	0.0062(6)	1O
O(7)	0.5171(5)	0.75	0.1692(4)	0.0091(6)	1O
O(8)	0.5105(5)	0.25	0.2948(4)	0.0091(6)	1O
O(9)	0.6490(6)	0.25	0.1087(4)	0.0183(9)	1O
O(10)	0.0736(5)	0.25	0.4234(4)	0.0063(6)	1O
H(1)	0.037(9)	0.25	0.333(8)	0.000(15)*	1H

* isotropic displacement factors.

Mg; M(2) = Al; and M(3) = Al, Fe^{3+}, Mn^{3+}. The most dominant elements in the A and M sites of the epidote group minerals are summarized in Table 8. From the viewpoint of crystal chemistry, niigataite corresponds to the Sr-analogue of clinozoisite or the Al-analogue of strontiopiemontite.

Another member with the highest Sr content in the epidote group is strontiopiemontite. For example, the amounts of SrO in the materials from the manganese deposit of Val Graveglia, Liguia, Italy (Bonazzi et al., 1990) and the Shiromaru mine, Tokyo, Japan (Kato and Matsubara, 1986) are 13.45 wt% (0.68 pfu) and 17.51 wt% (0.92 pfu), respectively. The present niigataite contains up to 16.33 wt% SrO (0.80 pfu).

Table 7. Interatomic distances (Å) of niigataite

A(1)-O(7)	2.252(4)		*A*(2)-O(7)	2.364(4)			
A(1)-O(3)	2.379(3)	x 2	*A*(2)-O(3)	2.572(3)	x 2		
A(1)-O(5)	2.487(4)		*A*(2)-O(2)	2.603(3)	x 2		
A(1)-O(1)	2.517(3)	x 2	*A*(2)-O(10)	2.661(4)			
A(1)-O(6)	2.736(4)		*A*(2)-O(2)	2.786(3)	x 2		
A(1)-O(9)	2.9462(18)	x 2	*A*(2)-O(8)	3.0402(18)	x 2		
<*A*(1)-O>	2.573		<*A*(2)-O>	2.703			
M(1)-O(4)	1.846(2)	x 2	*M*(2)-O(10)	1.851(2)	x 2	*M*(3)-O(8)	1.799(4)	
M(1)-O(1)	1.932(2)	x 2	*M*(2)-O(3)	1.864(3)	x 2	*M*(3)-O(4)	1.879(4)	
M(1)-O(5)	1.943(2)	x 2	*M*(2)-O(6)	1.934(2)	x 2	*M*(3)-O(2)	1.936(3)	x 2
<*M*(1)-O>	1.907		<*M*(2)-O>	1.883		*M*(3)-O(1)	2.166(3)	x 2
						<*M*(3)-O>	1.980	
Si(1)-O(7)	1.559(4)		Si(2)-O(8)	1.594(4)		Si(3)-O(2)	1.627(3)	x 2
Si(1)-O(9)	1.629(4)		Si(2)-O(3)	1.618(3)	x 2	Si(3)-O(6)	1.646(4)	
Si(1)-O(1)	1.655(3)	x 2	Si(2)-O(9)	1.620(4)		Si(3)-O(5)	1.657(4)	
<Si(1)-O>	1.625		<Si(2)-O>	1.613		<Si(3)-O>	1.639	
O(10)-H(1)	0.84(7)							

Niigataite is isostructural with the other members of epidote group minerals. A single chain of *M*(2) octahedra and a zigzag chain of *M*(1) and *M*(3) octahedra are connected with diortho groups of Si(1) and Si(2) tetrahedra and isolated Si(3) tetrahedra, forming a three-dimensional framework. Iron atoms have a tendency to occupy the largest *M*(3) site among the three octahedral sites, as those in the other members of epidote group minerals. As suggested by Dollase (1971), the larger Sr atoms selectively occupy the *A*(2) site which has a larger capacity with higher coordination number than the *A*(1) site in Niigataite, in analogy with those in strontiopiemontite (Bonazzi et al., 1990), and Pb atoms in hancockite (Dollase, 1971).

The cell volume of niigataite is relatively small among the epidote group minerals (Table 8 and Fig. 3), although this mineral contains a considerable amount of large Sr^{2+} ions in substitution for Ca^{2+} and Ce^{3+}. The length of *b* axis of solid solution between piemontite and androsite-(La) is linearly related with the sum of volumes of three octahedral *M* sites (Bonazzi et al., 1996). This correlation can be extended to the other members of epidote group minerals (Fig. 4). All of the three octahedral *M* sites in niigataite and those of clinozoisite are occupied by Al^{3+} which is the smallest among the octahedral ions in the epidote structure, *i.e.*, Al^{3+}(0.53), Fe^{3+}(0.55), Mn^{3+}(0.58), Fe^{2+}(0.61), V^{3+}(0.64), Mn^{3+}(0.67), Mg^{2+}(0.72); the values in parentheses are effective ionic radii in Å (Shannon and Prewitt, 1969, 1970). Consequently, the small octahedra in niigataite and clinozoisite result in shortening of the *b* axes. On the other hand, an effect of the difference in the size of the *A* cations, such as Ca^{2+}, Ce^{3+}, Sr^{3+}, Pb^{2+}, is observed on the value of

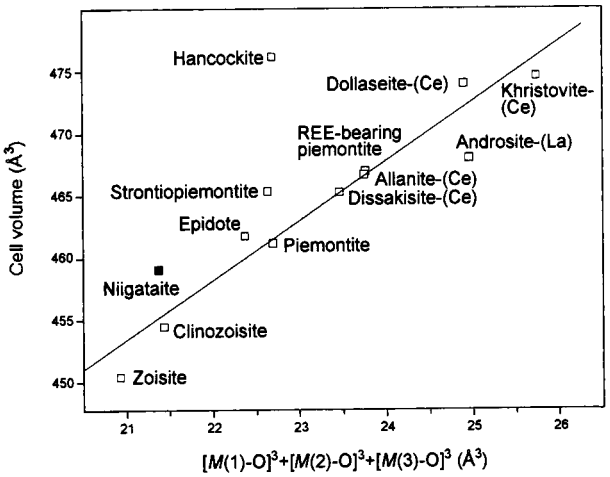

Figure 3. Correlation between the cell volume and the sum of cubes of mean *M*-O distances. The solid line represents the least square regression line for all the minerals except the Sr- and Pb-members, niigataite, strontiopiemontite and hancockite.

c·sinβ (Fig. 5), as suggested by Bonazzi et al. (1990). The mean *A*(2)-O distances and values of c·sinβ of the Sr-analogue, niigataite and strontiopiemontite are longer than those of the corresponding Ca-members, clinozoisite and piemontite, respectively. Bonazzi et al. (1990) also pointed out that the *A*(1)-O(7) distance decreases with the entry of larger Sr into the *A*(2) site. Figure 6 shows the relation of interatomic distances between *A*(1)-O(7) and *A*(2)-O(7). The rare earth elements (REE)-free members of epidote group minerals, *i.e.*, niigataite, clinozoisite, epidote and hancockite and almost REE-free piemontite (see the content of rare earth elements, C_{REE}, in Table 8) show a negative correlation. The REE-members of epidote group minerals

Table 8. The comparison of crystallographic data for epidote group minerals with general formula $A(1)A(2)M(1)M(2)M(3)(Si_2O_7)(SiO_4)O(OH)$

	a (Å)	*b* (Å)	*c* (Å)	β (°)	*V* (Å^3)	C_{REE}*
Niigataite[1]	8.882(3)	5.5906(16)	10.210(2)	115.118(18)	459.1(2)	0.00
Clinozoisite[2]	8.872(1)	5.593(1)	10.144(1)	115.46(1)	454.5(1)	0.00
Epidote[3]	8.903(2)	5.649(1)	10.163(1)	115.39(1)	461.8(1)	0.00
Hancockite[4]	8.958(20)	5.665(10)	10.304(20)	114.4(4)	476.2	0.00
Allanite-(Ce)[5]	8.894(1)	5.724(1)	10.102(1)	114.87(1)	466.6(1)	0.80
Piemontite[6]	8.857(1)	5.671(1)	10.156(1)	115.29(1)	461.2(1)	0.05
REE-bearing piemontite[7]	8.890(2)	5.690(1)	10.135(2)	114.44(2)	466.7(2)	0.50
Strontiopiemontite[8]	8.849(2)	5.671(2)	10.203(2)	114.63(2)	465.4(2)	0.00
Dissakisite-(Ce)[9]	8.905(1)	5.684(1)	10.113(1)	114.62(2)	465.3†	1.00
Mukhinite[10]	8.90	5.61	10.15	115.50	457	
Khristovite-(Ce)[11]	8.903(6)	5.748(3)	10.107(7)	113.41(5)	477.6(2)	0.94
Androsite-(La)[12]	8.896(1)	5.706(1)	10.083(1)	113.88(1)	468.0(1)	0.72
Dollaseite-(Ce)[13]	8.934(18)	5.721(7)	10.176(22)	114.31(12)	474.0	0.98
Zoisite[14]	16.1909(15)	5.5466(5)	10.0323(6)	——	450.47(8)x2	

Mean interatomic distances (Å)	*A*(1) <*A*(1)-O>$_9$	*A*(2) <*A*(2)-O>$_{10}$	*M*(1) <*M*(1)-O>$_6$	*M*(2) <*M*(2)-O>$_6$	*M*(3) <*M*(3)-O>$_6$	Crystal system	Space group
Niigataite[1]	Ca 2.573	Sr 2.703	Al 1.907	Al 1.883	Al 1.980	Monoclinic	$P2_1/m$
Clinozoisite[2]	Ca 2.576	Ca 2.671	Al 1.904	Al 1.880	Al 1.990	Monoclinic	$P2_1/m$
Epidote[3]	Ca 2.593	Ca 2.678	Al 1.920	Al 1.885	Fe^{3+} 2.048	Monoclinic	$P2_1/m$
Hancockite[4]	Ca 2.60†	Pb 2.75†	Al 1.94†	Al 1.88†	Fe^{3+} 2.06†	Monoclinic	$P2_1/m$
Allanite-(Ce)[5]	Ca 2.602	REE 2.672	Al 1.933	Al 1.892	Fe^{2+} 2.134	Monoclinic	$P2_1/m$
Piemontite[6]	Ca 2.589	Ca 2.680	Al 1.931	Al 1.885	Mn^{3+} 2.064	Monoclinic	$P2_1/m$
REE-piemontite[7]	Ca 2.589†	Ca 2.688	Al 1.968	Al 1.889	Mn^{3+} 2.109	Monoclinic	$P2_1/m$
Strontiopiemontite[8]	Ca 2.578	Sr 2.712	Al 1.929	Al 1.885	Mn^{3+} 2.061	Monoclinic	$P2_1/m$
Dissakisite-(Ce)[9]	Ca 2.598†	REE 2.676†	Al 1.941	Al 1.890	Mg 2.110	Monoclinic	$P2_1/m$
Mukhinite[10]	Ca —	Ca —	Al —	Al —	V —	Monoclinic	$P2_1/m$
Khristovite-(Ce)[11]	Ca 2.59	REE 2.70	Mn^{3+} 2.01	Al 1.91	Mn^{2+} 2.20	Monoclinic	$P2_1/m$
Androsite-(La)[12]	Mn 2.577†	REE 2.686	Mn^{3+} 2.010	Al 1.892	Mn^{2+} 2.159	Monoclinic	$P2_1/m$
Dollaseite-(Ce)[13]	Ca 2.607†	REE 2.691†	Mg 2.028	Al 1.902	Mg 2.131	Monoclinic	$P2_1/m$
Zoisite[14]	Ca 2.5613†	Ca 2.6851†	Al 1.8882	Al 1.8882	Al 1.9541	Orthorhombic	*Pnma*

*Rare earth elements content per formula unit.

†Recalculated from the literature data by the present authors with UMBADTEA (Finger, 1968), PC/DOS-version (Horiuchi, personal communication). [1]Present study, [2] CH in Bonazzi and Menchetti (1995), [3]MBN in Bonazzi and Menchetti (1995), [4]Dollase (1971), 5SN3 in Bonazzi and Menchetti (1995), [6]BR2P in Bonazzi et al. (1992), [7]VA-1a in Bonazzi et al. (1996), [8]SRPM in Bonazzi et al. (1990), [9]Rouse and Peacor (1993), 10ICDD #22-1066 (after Shepel and Karpenko, 1969), [11]Pautov et al. (1993); Sokolova et al. (1991), [12]AND-517 in Bonazzi et al. (1996), [13]Peacor and Dunn (1988), [14]Smith et al. (1987).

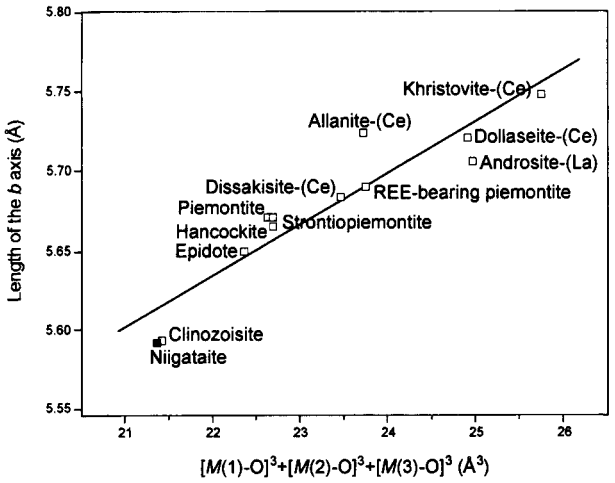

Figure 4. Diagram showing the linear relation between the length of *b* axis and the sum of cubes of mean *M*-O distances. The solid line represents the least square regression line for all the minerals.

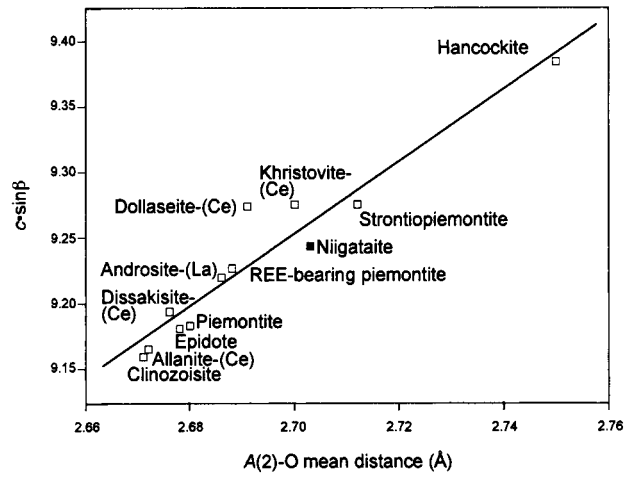

Figure 5. The value of c·sinβ plotted vs. the mean A(2)-O distance. The solid line represents the least square regression line for all the minerals.

with $C_{REE} \geq 0.8$, allanite-(Ce), dollaseite-(Ce), dissakisite-(Ce) and khristovite-(Ce) have a different trend. The REE-bearing piemontite ($C_{REE} = 0.50$ in Table 8) can be plotted on the intermediate position between the two trends in Figure 6. Androsite-(La) can be plotted on the trend of REE-free members, although it is a REE-member ($C_{REE} = 0.72$). A specific difference of androsite-(La) from the other members is the occupation of Mn in the A(1) site instead of Ca. The ionic radius of Mn is approximately 0.02 Å smaller than that of Ca. The difference in the size of ion in the A(1) site directly affects the A(1)-O(7) distance. Consequently, the A(1)-O(7) distance of androsite-(La) is shortened as indicated by the arrow shown in Figure 6. The shrinkage of A(1)-O(7) in the direction of c·sinβ makes the change in the value of c·sinβ provokes a slight change in c·sinβ accompanying the entry of larger Sr atoms in the A(2) site.

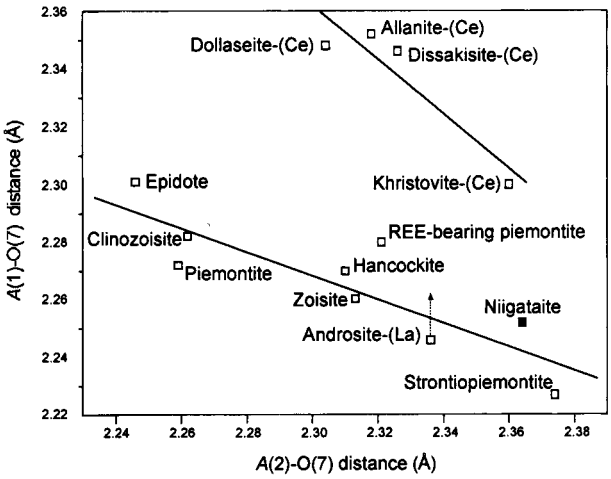

Figure 6. Trends of the A(1)-O(7) distance as a function of A(2)-O(7) distance. The upper line represents the regression line derived from REE-members, allanite-(Ce), dollaseite-(Ce), dissakisite-(Ce) and khristovite-(Ce). The lower line represents the regression line derived from the monoclinic REE-free members. The arrow indicates the difference between Ca-O and Mn-O distances for the A(1)-O(7) sites approximated from the individual ionic radii.

Sr container in subducted slab

The epidote group minerals and lawsonite are regarded as the most important Sr containers in subducted slab and serving as a Sr carrier to the mantle (Enami, 1999). Zoisite and epidote, which contain up to 3.2 wt% SrO, are common constituents of eclogites and associated paraschists throughout the Su-Lu ultra high pressure province, eastern China (Nagasaki and Enami, 1998). Epidote, which contains up to 8.5 wt% SrO, was reported in metagreywacke-quartzofelspathic schist from Southern Alps, New Zealand (Grapes and Watanabe, 1984). In addition, epidote with up to 10.3 wt% SrO was found in metabasite from the Motagua Fault Zone, Guatemala (Harlow, 1994). The site occupancies of Sr in the A(2) site are 14 % (China), 39 % (New Zealand) and 53 % (Guatemala). In the case of the present niigataite, the occupancy of Sr in A(2) site reaches 72 % (Table 6). These results indicate that Sr can be accommodated as a major component in the A(2) site of the epidote group minerals.

Genetical consideration

The bulk compositions of rodingite, jadeitite and albitite, which are also tectonic blocks in serpentinite melange from the Itoigawa-Ohmi district, are given in Table 3. The bulk chemical composition of the niigataite-bearing prehnite rock resembles that of rodingite.

The host rock of niigataite is composed mainly of prehnite, with subordinate amounts of diaspore, Sr-bearing clinozoisite, chlorite and niigataite. It is characterized by extraordinarily coarse-grained prehnite crystals and abundant occurrence in druse. These features support that the host rock of niigataite was recrystallized in solution on the stage of formation of the serpentinite melange. The crystallization of prehnite is followed by formation of diaspore, niigataite and chlorite. Calcium atoms in prehnite occupy the sevenfold-coordinated sites (Zunic et al., 1990). The mean bond distance of Ca-O in prehnite is 2.47 Å which is almost identical to the sum of effective ionic radii of Ca (1.07Å) and O (1.40Å) (Shannon and Prewitt, 1969). The effective ionic radius of sevenfold-coordination of Sr (1.21Å) (Shannon and Prewitt, 1969) appears to be slightly too long for Sr to replace Ca in prehnite. The larger tenfold-coordinated *A*(2) site of clinozoisite can readily accept not only Sr (1.36Å), but also Ca (1.23Å). The extremely low Sr content in prehnite, which is below the detection limit of the EDS-analysis, accounts for the crystallochemical exclusion of Sr from the prehnite structure. Thus recrystallization of prehnite from solution should cause concentration of Sr in residual liquid. From these results and consideration, it is concluded that niigataite is formed from the Sr-rich residual liquid in the later stage of the formation of the prehnite rock.

Recently, three new Sr silicate minerals have been found from jadeitites in this district: itoigawaite $SrAl_2Si_2O_7(OH)_2{\cdot}H_2O$ (Miyajima et al., 1999), rengeite $Sr_4ZrTi_4(Si_2O_7)_2O_8$ (Miyajima et al., 2001) and matsubaraite $Sr_4Ti_5(Si_2O_7)_2O_8$ (Miyajima et al., 2002). Moreover, Sr-dominant minerals such as stronalsite $Na_2SrAl_4Si_4O_{16}$, slawsonite $SrAl_2Si_2O_8$, lamprophyllite $Sr_2Na_3Ti_3(Si_2O_7)_2(O,OH,F)$, thomsonite-Sr $NaSr_2Al_5Si_5O_{20}{\cdot}6H_2O$, tausonite $SrTiO_3$ and strontium-apatite $Sr_5(PO_4)_3(OH,F)$ are found in jadeitites and albite-bearing jadeitite from this district. Albitite related to the genesis of jadeite also include ohmilite, $Sr_3TiSi_4O_{12}(O,OH){\cdot}2\text{-}3H_2O$, (Komatsu et al., 1973), strontio-orthojoaquinite, $Na_{2+x}Ba_4Fe_{1.5}(Sr, Ba, REE, Nb)_{4-x}Ti_4(O,OH)_4(Si_4O_{12})_4{\cdot}2H_2O$, (Wise, 1982; Chihara et al., 1974), and strontium-apatite (Sakai and Akai, 1994). Although many species of Sr-dominant minerals have been found in jadeitites and albitites in serpentinite melange, they have not been found in both schists as tectonic blocks in the serpentinite melange and the host serpentinite to date. The formation of Sr-dominant minerals is restricted to jadeitite, albitite and Ca-Al silicate rocks such as rodingite and prehnite rock. This indicates that the original materials and metamorphic processes are different between schists and the other metamorphic rocks.

Acknowledgements

The first author is grateful to Emeritus Prof. K. Aoki of Tohoku University, Prof. M. Enami of Nagoya University, Prof. K. Kunugiza of Toyama University, Mr. F. Matsuyama of the University of Tokyo, and Dr. T. Oba of Joetsu University of Education for their discussion and encouragement. He would like to thank Miss M. Kubota for her help to XRF analyses. Special thanks are extended to Prof. H. Horiuchi of Hirosaki University, Prof. Y. Nakamuta of Kyushu University and for Dr. K. Sugiyama of the University of Tokyo for their offers of their computer programs, for their permission to apply them, and for their suggestion on the XRD investigations. The authors are gratefully to Prof. I. Kusachi of Okayama University, Prof. K. Tomeoka and an anonymous reviewer of journal for their constructive comments and suggestions. A part of this work is supported by a Grant-in-Aid for Scientific Research from Japan Society for the Promotion of Science (#11916021).

References

Bonazzi, P., Menchetti, S. and Palenzona, A. (1990) Strontiopiemontite, a new member of the epidote group, from Val Graveglia, Italy. European Journal of Mineralogy, 2, 519-523.

Bonazzi, P., Garbarino, C. and Menchetti, S. (1992) Crystal chemistry of piemontite: REE-bearing piemontite from Monte Brugiana, Alpi Apuane, Italy. European Journal of Mineralogy, 4, 23-33.

Bonazzi, P. and Menchetti, S. (1995) Monoclinic members of the epidote group: effects of the $Al \rightleftharpoons Fe^{3+} \rightleftharpoons Fe^{2+}$ substitution and of the entry of REE^{3+}. Mineralogy and Petrology, 53, 133-153.

Bonazzi, P., Menchetti, S. and Reinecke, T. (1996) Solid solution between piemontite and androsite-(La), a new mineral of the epidote group from Andros Island, Greece. American Mineralogist, 81, 735-742.

Chihara, K., Komatsu, M. and Mizota, T. (1974) A joaquinite-like mineral from Ohmi, Niigata Prefecture, central Japan. Mineralogical Journal, 7, 395-399.

Deer, W. A., Howie, R. A. and Zussman, J. (1997) Rock forming minerals. 1B, Disilicates and ring silicates. pp.629, The Geological Society, London.

Dollase, W. A. (1968) Refinement and comparison of the structure of zoisite and clinozoisite. American Mineralogist, 53, 1882-1898.

Dollase, W. A. (1971) Refinement of the crystal structure of epidote, allanite and hancockite. American Mineralogist, 56, 447-464.

Enami, M. (1999) CaAl-silicates: An important Sr container in subducted slab. Journal of Geography, 108, 177-187(in Japanese).

Finger, L. W. (1968) *UMBADTEA*. Program for computing bond angles and distances, and thermal ellipsoids with error analysis. University of Minnesota, U.S.A.

Grapes, R. and Watanabe, T. (1984) Al-Fe^{3+} and Ca-Sr^{2+} epidotes in the meta-greywacke-quartzofeldspathic schist, Southern Alps, New Zealand. American Mineralogist, 69, 490-498.

Harlow, G. E. (1994) Jadeitites, albitites and related rocks from the Motagua Fault Zone, Guatemala. Journal of Metamorphic

Geology, 12, 49-68.

International Tables for Crystallography, Volume C (1992) Wilson, A.J.C. Ed., Kluwer Academic Publishers, Dordrecht.

Kato, A. and Matsubara, S. (1986) Strontian piemontite. Abstracts of 1986 Joint Annual Meeting of The Society of Resource Geology, The Japanese Association of Mineralogists, Petrologists and Economic Geologists, and The Mineralogical Society of Japan, B3, 69 (in Japanese).

Kawano, Y. (1939) A new occurrence of jade (jadeite) in Japan and its chemical properties. Journal of Japanese Association of Mineralogy, Petrology and Economic Geology, 22, 195-201. (in Japanese)

Komatsu, M. (1990) Hida "Gaien" Belt and Joetsu Belt. In Pre-Cretaceous terranes of Japan (Ichikawa, K. et al. Eds.). pp.224, Publication of IGCP Project, 25-40.

Komatsu, M., Chihara, K. and Mizota, T. (1973) A new strontium-titanium hydrous silicate mineral from Ohmi, Niigata Prefecture, central Japan. Mineralogical Journal, 7, 298-301.

Macicek, J. (1991) Bulgarian Academy of Sciences, Sofia, Bulgaria, ICDD Grant-in-Aid, ICDD#44-1400.

Miyajima, H., Matsubara, S., Miyawaki, R. and Ito, K. (1999) Itoigawaite, a new mineral, the Sr analogue of lawsonite, in jadeitite from the Itoigawa-Ohmi district, central Japan. Mineralogical Magazine, 63, 906-916.

Miyajima, H., Matsubara, S. Miyawaki, R. and Hirokawa, K. (2001) Rengeite, $Sr_4ZrTi_4Si_4O_{22}$, a new mineral, the Sr-Zr analogue of perrierite from the Itoigawa-Ohmi district, Niigata Prefecture, central Japan. Mineralogical Magazine, 65,111-120.

Miyajima, H., Miyawaki, R. and Ito, K. (2002) Matsubaraite, $Sr_4Ti_5Si_4O_{22}$, a new mineral, the Sr-Ti analogue of perrierite in jadeitite from the Itoigawa-Ohmi district, Niigata Prefecture, Japan. European Journal of Mineralogy, 14, 1119-1128.

Murata, M. (1993) Major and trace component analysis of Korean Institute of energy and Resource igneous rock reference samples using X-ray fluorescence spectrometer. Research Bulletin of Natural Science, Naruto University of Education, 8, 37-49.

Nagasaki, A. and Enami, M. (1998) Sr-bearing zoisite and epidote in ultra-high pressure (UHP) metamorphic rocks from the Su-Lu province, eastern China: An important Sr reservoir under UHP conditions. American Mineralogist, 93, 240-247.

Nakajima, T., Ishiwatari, A., Sano, S., Kunugiza, K., Okamura, M., Kano, T., Soma, T. and Hayasaka, Y. (1992), Geotraverse across the Southwest Japan Arc: an overview of tectonic setting of Southwest Japan. In 29th IGC Field Trip Guide Book, vol.5: Metamorphic belts and related plutonism in the Japanese Islands (Kato, H. and Noro, H. Eds.). pp. 361, Geological Survey of Japan, A25, 1-83.

Nakamuta, Y. (1999) Precise analysis of a very small mineral by an X-ray diffraction method. Journal of the Mineralogical Society of Japan, 28, 117-121 (in Japanese with English abstract).

Nishimura, Y. (1998) Geotectonic subdivision and areal extent of the Sangun belt, Inner Zone of Southwest Japan. Journal of Metamorphic Geology, 16, 129-40.

Pautov, L. A., Khorov, P. V., Ignatenko, K. I., Sokolova, E. V. and Nadezhina, T. N. (1993) Khristovite-(Ce) - (Ca,REE) REE $(Mg,Fe)AlMnSi_3O_{11}(OH)(F,O)$: A new mineral in the epidote group. Zapiski Vserossii skogo Mineralogicheskogo Obshchaestva (Proceedings of the Russian Mineralogical Society), 122, 103-111 (in Russian).

Peacor, D. R. and Dunn, P. J. (1988) Dollaseite-(Ce) (magnesium orthite redefined): Structure refinement and implications for $F + M^{2+}$ substitutions in epidote-group minerals. American Mineralogist, 73, 838-842.

Rouse, R. C. and Peacor, D. R. (1993) The crystal structure of dissakisite-(Ce), the Mg analogue of allanite-(Ce). Canadian Mineralogist, 31, 153-157.

Sakai, M. and Akai, J. (1994) Strontium, barium and titanium-bearing minerals and their host rocks from Ohmi, Japan. Science Report of Niigata University, Series E (Geology and Mineralogy), 9, 97-118.

Shannon, R. D. and Prewitt, C. T. (1969) Effective ionic radii in oxides and fluorides. Acta Crsytallographica, B25, 925-46.

Sheldrick, G. M. (1997) SHELXL-97. Program for crystal-structure refinement. University of Göttingen, Germany.

Shepel, A. V. and Karpenko, M. V. (1969) Mukhinite, a new vanadium species of epidote. Doklady of the Academy of Sciences of the U.S.S.R., Earth Science Sections, 185, 123-126.

Smith, J. V., Pluth, J. J., Richardson, J. W. Jr. and Kvick, Å. (1987) Neutron diffraction study of zoisite at 15 K and X-ray study at room temperature. Zeitschrift für Kristallographie, 179, 305-321.

Sokolova, E. V., Nadezhina, T. N. and Pautov, L. A. (1991) Crystal structure of a new natural silicate of manganese from the epidote group. Soviet Physics, Crystallography, 36, 172-174 (translated from Kristallografiya, 36, 330-333).

Toraya, H. (1993) The determination of unit-cell parameters from Brag reflection data using a standard reference material but without a calibration curve. Journal of Applied Crystallography, 26, 583-590.

Wise, S. W. (1982) Strontiojoaquinite and barrio-orthojoaquinite: two new members of the joaquinite group. American Mineralogist, 67, 809-816.

Zunic, T. B., Scavnicar, S. and Molin G. (1990) Crystal structure of prehnite from Komiza. European Journal of Mineralogy, 2, 731-734.

Manuscript received; 3 February, 2003
Manuscript accepted; 24 June, 2003